

Cell Deformability Studies for Clinical Diagnostics: Tests with Blood Analogue Fluids using a Drop based Microfluidic Device

A. S. Moita¹, C. Caldeira¹, F. Jacinto¹, R. Lima^{2,3}, E. J. Vega⁴ and A. L. N. Moreira¹

¹IN⁺ Center for Innovation, Technology and Policy Research, Instituto Superior Técnico, Universidade de Lisboa, Av. Rovisco Pais, 1049-001, Lisboa, Portugal

²CEFT, Faculdade de Engenharia da Universidade do Porto (FEUP), R. Dr. Roberto Frias, 4200-465, Porto, Portugal

³Metrics, Mechanical Engineering Department, University of Minho, Campus de Azurém, 4800-058, Guimarães, Portugal

⁴Área de Mecánica de Fluidos, Dpto. de Ingeniería Mecánica, Energética y de los Materiales, Escuela de Ingenierías Industriales, Universidade de Extremadura, Campus Universitario, Av. de Elvas, s/n, 06006, Badajoz, Spain

Keywords: Lab-on-a-chip, Droplet based Microfluidics, Clinical Diagnostics, Cell Deformability, Bioanalogue Fluid.

Abstract: The present paper addresses the final tests (concerning the transport section) of a microfluidic device to be used in cancer diagnostics, based on the mechanical properties of the cells and particularly on deformability. Following the previous work, which established the materials to be used, according to the wetting properties and their influence on the dynamic response of the droplets (which are electrostatically actuated) this paper presents the final simulations to optimize the thickness and material of the dielectric coating, always as a function of the dynamic response of the droplets. Then, to avoid contamination issues, a number of analogue fluids are proposed, in a new approach, which are characterized and tested in the second part of the work. Regarding the characterization of these new fluids, preliminary results suggest a great potential of a surfactant solution to be used as an analogue. The addition of the surfactant results in the formation of semi-rigid particles with a size distribution and deformation characteristics compatible with those of the biosamples to be studied. The surfactant solution also shows a swift response to electrostatic actuation.

1 INTRODUCTION

Lab-on-chip devices are pointed as strongly effective tools to perform a number of complex sample manipulation operations, biochemical analysis and immunoassay tests (e.g. Takahashi *et al.*, 2004, Gossett *et al.*, 2010, Shields *et al.*, 2015, Chim, 2015). Besides allowing a significant reduction of the samples and of the reagents as well as a better control of the reactions, due to the small characteristic time and length scales, the microfluidic devices offer a significant energy reduction, are easy to use and portable. Furthermore, errors and contamination issues are precluded, since the manual handling is marginal (Lin *et al.*, 2010).

Sample transport in continuous medium using microchannels is probably the most common microfluidic design, but addresses a number of inconveniences such as the need for auxiliary systems, which are still very ineffective from the energetic point of view, clogging, difficulties in accessing the samples, among others (Geng *et al.*,

2017). In this context, droplet-based microfluidics is considered by several authors as an effective alternative (e.g. Pollack *et al.*, 2011, Dance, 2017). Droplet handling can be performed using different kinds of external actuation, (e.g. Zeggari *et al.*, 2014) although electrowetting is amongst the most popular and well grounded. However, although theoretical background on electrowetting is already well recognized, as revised for instance in Mugele and Baret (2005) and more recently in Nelson *et al.* (2012) the details required for an effective design and assembly of the chips is scarcely reported in the literature (e.g. Li *et al.*, 2012). Hence, optimization of the chip design requires a deep knowledge on the wetting properties of the materials used (e.g. Chim, 2015, Vieira *et al.*, 2017), as well as an accurate description of biosamples fluid dynamics and response under external actuation (e.g. Moita *et al.*, 2016).

Microfluidic devices are also suitable to take advantage of particular properties of the biosamples, towards the development of label free diagnostic approaches. In this context, mechanical properties of

the cells and particularly their deformability are a hallmark to identify several diseases, such as cancer. Characterizing cancer cell deformation can provide useful information on the process of metastasis, particularly for large deformability regimes, which are rarely described in the literature (Hu *et al.*, 2018). Furthermore, a few authors have drafted preliminary correlations between the deformability ratio of the cells and the stage of malignancy (e.g. Tse *et al.*, 2013). At the microscale, it is also expected that droplet dynamics can be sensitive to the rheological variations caused by different degrees of cell stiffness/deformability, so droplet dynamics could be eventually correlated with cell stiffness for early stage cancer diagnostics (e.g. Vieira *et al.*, 2017).

Following our previous work (Jacinto *et al.*, 2018), the present paper focuses on the development of a droplet based microfluidic system, intended to be used in clinical diagnostics (lung cancer) based on cell deformability and its possible correlation with the fluid dynamics of the droplets used for the sample handling. The paper is organized in two main sections: the first summarizes the process of design and optimization of the lab-on-chip device, whose configuration (electrodes dimensioning and positioning, materials and wetting properties) were optimized based on the dynamic behavior (spreading, contact diameter and velocity) of the biosample droplets. Then, following an original approach, a brief description is made on the procedure which will be used to infer on a possible correlation between the cells deformability and different stages of malignancy, following the work of Tse *et al.* (2013). It is worth mentioning that at this stage of the work, analogue fluids are proposed to be used in the preliminary assays, to overcome contamination issues, among others. Within this scope, different approaches are considered in the present work, to devise the analogue fluids, namely, using xanthan gum solutions and suspensions of polymers and surfactants solved on water, giving rise to small semi-rigid particles. The main physical properties of the fluids are accessed and they are characterized in terms of the resulting particle size distribution, evaluated based on Laser Scanning Fluorescence Confocal Microscopy. The size and deformability of the resulting particles is then tested to check on their feasibility to mimic cell deformability in the context of the current main goal of this work (malignancy diagnostics). The dynamic response of the analogue fluids is also tested to check on the feasibility of their handling in the microfluidic device.

2 MATERIALS AND METHODS

2.1 Numerical Method

In our previous work, the materials used to assemble the microfluidic device were carefully selected, based on their wetting properties and on an intensive analysis to minimize adsorption issues, which were affecting sample handling, besides being an obvious source of contamination (Vieira, *et al.*, 2017, Moita *et al.*, 2018). A numerical approach was then followed to predict the motion of the sample microdroplets, optimizing the chip configuration to promote droplet motion (Jacinto *et al.*, 2018). Following these steps, a final numerical optimization was performed to check on the correct selection of the dielectric materials which are used to coat the electrodes. Their thickness is also optimized, to maximize the resulting electrostatic force, the distance travelled by the droplet and the velocity of the moving droplets. These parameters were optimized for the lowest possible applied voltage.

The numerical study was performed using COMSOL Multiphysics 4.3b. The electrostatic forces actuating on the droplets were determined using Maxwell stress tensor, integrated on droplets' surface.

Droplet motion was simulated using an incompressible formulation of Navier-Stokes equations for a laminar flow. Phase Field User Interface was used to track the liquid-air interface. The complete model formulation together with the detailed description of the computational domain and boundary conditions used can be found in Jacinto *et al.* (2018).

2.2 Experimental Method

An experimental approach, as proposed in the present work, was followed to characterize the analogue fluids and check on their suitability to infer on possible correlations between the deformability of the cells and different stages of malignancy. The analogue fluids were characterized in terms of their main physico-chemical properties and on the size distribution of the particles mimicking the cells, as described in the following sub-sections. The electrostatic response of the various analogue fluids tested here was also inferred, using the experimental arrangement detailed below.

2.2.1 Experimental Arrangement

The dynamic response of the analogue fluids was evaluated on a simplified arrangement. In this

arrangement, a 25 μm diameter tungsten wire (Goodfellow Cambridge Ltd), acting as an electrode, was dipped inside the droplet to be tested. The counter electrode on which the droplet was deposited was a copper cylinder with 19mm of diameter and 20mm height. A 10 μm Teflon film (Goodfellow Cambridge Ltd) was used as the dielectric layer. As recommended by Restolho *et al.* (2009), a very thin film of sodium chloride was placed between the counter electrode and the dielectric to avoid the presence of an air gap. Both electrodes were connected to a Sorensen DCR600-.75B power supply and DC voltage was applied. The tests were performed inside a Perspex chamber with quartz windows to avoid optical distortion, under continuously controlled temperature and relative humidity conditions. The chamber was previously saturated with the working fluid, for each fluid used. Relative humidity measurements were taken at a sample rate of 0.5Hz, with an accuracy of 2-5%. Temperature measurements were taken also at a sample rate of 0.5Hz, within $\pm 0.5^\circ\text{C}$ accuracy. Measurements were performed using a DHT 22 Humidity & Temperature Sensor. The temperature was observed to be constant within $T=20\pm 3^\circ\text{C}$ and relative humidity was kept constant between 75% and 78%. This entire set-up was directly mounted on an optical tensiometer THETA, from Attention. Using the sessile drop method, the equilibrium contact angle (the angle formed in equilibrium, between the surface line and a tangent line touching droplet edge) was evaluated as a function of the applied voltage, for a range between 0-230V in 25V increments. The final curves presented and discussed here were averaged from at least six assays, obtained under similar conditions. Droplet volume was kept constant and equal to 3 μl .

The detailed description of the set-up (with the appropriate schematics) and experimental procedures which were used here to access the dynamic response of the analogue fluids under electrostatic actuation can be found in Moita *et al.* (2016).

2.2.2 Preparation of the Analogue Fluids and Characterization of their Physico-chemical Properties

Analogue fluids were prepared following three different strategies, namely using xanthan gum, using a suspension of polymeric particles in water DD and mixing water DD with a small quantity of surfactant which results in the formation of semi-rigid surfactant particles.

The xanthan gum solutions were prepared with

the concentrations of 0.05wt% and 0.35wt%. As these solutions have a shear thinning behaviour, the viscosity vs shear rate curves were fitted using the Cross model (Cross, 1965), following the procedure described in Moita *et al.* (2015). Rheological data were measured under controlled temperature conditions, at ATS RheoSystems (a division of CANNON® Instruments, Co). The accuracy of the measurements is within $\pm 5\%$. The suspensions of polymeric particles were prepared with PMMA - Poly(methyl methacrylate) dissolved in water DD (1wt%). Different concentrations are expected to be tested in the near future. Seeking at appropriate characteristic spatial scales that could be used to mimic the cells, different particle diameters were tested here, namely 5 μm , 10 μm and 20 μm . Finally, the third approach consisted in adding a surfactant Brij40 (a nonionic polyoxyethylene surfactant from Thermo Fisher) which results in the formation of semi-rigid micro-particles suspended in the water.

Surface tension σ_v was measured using the optical tensiometer (THETA from Attention). The final surface tension values were averaged from 15 measurements taken under controlled temperature conditions ($20\pm 3^\circ\text{C}$). Measurements have standard mean errors always lower than 0.35. Density ρ was measured with a pycnometer for liquids and concentrations were checked by basic concentration calculations. The detailed description of the measurement procedures can be found in Moita *et al.* (2018). Table 1 summarizes the main physico-chemical properties of the various fluids tested here.

It is worth mentioning that varying the diameters of the PMMA particles did not produce any significantly quantifiable modification in the density or in the surface tension of the fluids tested here.

Table 1: Density and surface tension (measured at room temperature $20\pm 3^\circ\text{C}$) of the analogue fluids tested in the present work.

Solution	Density ρ [kg/m ³]	Surface tension σ_{lv} [mN/m]
Xanthan gum 0.05wt%	997	72.0
Xanthan gum 0.35wt%	997	72.95
Water DD + PMMA particles (1wt%)	999	58.65
Water DD + Brij40	999	21.10

2.2.3 Characterization of Particles Sizes and Deformability using Laser Scanning Fluorescent Confocal Microscopy

Analogue fluids were further characterized in terms of the size distribution of their particles and of their deformability capability (to mimic the various degrees of cell deformability associated to the different stages of malignancy). The analysis of the size distribution was performed based on extensive post-processing of images taken with a Laser Scanning Confocal Microscope (SP8 from Leica), using an in-house code developed in MATLAB. The images were taken using Rhodamine B (Sigma Aldrich) as fluorophore in a concentration of 3.968×10^{-6} g/ml, which does not alter the physico-chemical properties of the analogue fluids. A laser with 552 nm wavelength, was used. The power of the laser was set to 10.50 mW (3.00% of its maximum power) and the gain of the photomultiplier was fixed at 550V. These values were chosen after a sensitivity analysis on the contrast of the image (before the post-processing) and on the Signal to Noise Ratio (SNR). The images were recorded in the format 1024×1024 pixels² and the scanning frequency was set to 400 Hz. For the optical arrangement used, the lateral and axial resolutions for most of the measurements are $R_l = 0.375 \mu\text{m}$ and $R_a = 1.4 \mu\text{m}$, while the optical slice thickness was $2.2 \mu\text{m}$.

The deformability of the particles in the fluids was assessed by using a 2D microfluidic device (made of PDMS) composed of a microchannel with a hyperbolic shaped contraction, measuring at the end of this contraction (around the smallest cross-section) and visualizing the particles with a high-speed video microscopy system (high-speed camera connected to an inverted microscope), as in Pinho (2018).

3 RESULTS AND DISCUSSION

3.1 Design and Optimization of the Microfluidic Device

In Vieira *et al.* (2017) and later in Moita *et al.* (2018) a careful selection of the materials to assemble the microfluidic device was performed, addressing the wetting properties of the dielectric coating. This analysis, which was performed as a function of the dynamic response of the biofluid droplet under electrostatic actuation revealed the

paramount role of the wetting properties of the dielectric in allowing an efficient handling of the biosamples. Hence, besides the hydrophobicity, the reduced hysteresis to minimize energy dissipation at the droplet surface contact line showed to be a factor of major importance. Furthermore, minimizing adsorption was also shown to be relevant, not only to reduce contamination issues, but also to promote droplet motion. Indeed, Moita *et al.* (2018) clearly showed that the adsorption of the biocomponents (e.g. proteins) could lead to a local increase of the wettability, which would promote droplet spreading and energy dissipation at the contact line, thus limiting droplet continuous motion. In line with this and combining the electrical properties with the aforementioned wetting issues, Moita *et al.* (2018) recommend the use of PDMS (Polydimethylsiloxane) or Teflon coated with a commercial compound called Glaco[®], a perfluoroalkyltrichlorosilane combined with perfluoropolyether carboxylic acid and a fluorinated solvent (Kato *et al.*, 2008), to promote the superhydrophobicity of the dielectric, while reducing the adsorption of the biocomponents.

However, when designing the optimized electrodes configuration, also as a function of the dynamic response of the biosample droplets, Jacinto *et al.* (2018) noticed that the negative effect of an excessive increase of the thickness of the dielectric, according to Young-Lippmann equation, would reduce droplet motion, compromising the efficacy of the microfluidic chip. It is worth mentioning that the Young-Lippman equation states that the contact angle of the droplet under electrostatic actuation is proportional to the applied voltage and inversely proportional to the thickness of the dielectric. The detailed theoretical analysis on this and other basic principles of electrowetting is revised in Mugele and Baret (2005) and in Nelson and Kim (2012), for instance.

In line with this, for the specified dielectrics, an additional simulation was performed to optimize the thickness of the dielectric, maximizing the resulting electrostatic force, the distance travelled by the droplet and its velocity. Hence, Figure 1 depicts the numerical results on the maximum velocity of a droplet while moving on the chip for a time interval of 10ms, as a function of the thickness of the dielectric, for a fixed imposed voltage of 90V. Following the previous simulations (Jacinto *et al.*, 2018), the droplet is a biofluid (a solution of GFP – Green Fluorescent Protein, produced and purified in house, with 1.71×10^{-3} mM concentration) with an initial diameter of 1.3mm.

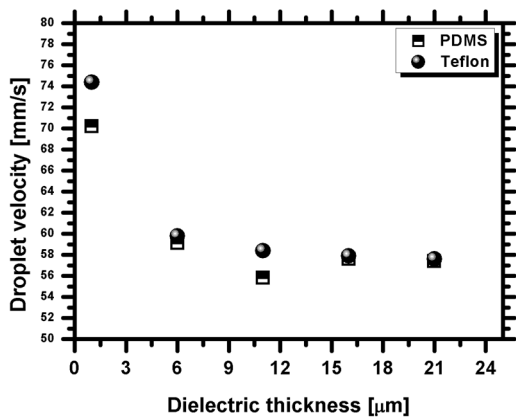


Figure 1: Maximum droplet velocity, as a function of the dielectric thickness, for different dielectric materials, and a fixed imposed voltage of 90V. The GFP droplet with 1.71×10^{-3} mM concentration has an initial diameter of 1.3mm.

The Figure clearly shows the maximization of droplet velocity, for a fixed reduced value of the imposed voltage, for a dielectric thickness of the order of 1-6 μ m. For thicker values, the droplet velocity becomes very low, as shown in the Figure and eventually the motion of the droplet is totally precluded. On the other hand, the thickness can be further tuned and eventually reduced within the nanometric scale, although in this case, the eventual benefits arriving for droplet transport are probably overcome by the difficulty and costs of the manufacturing process. Furthermore, for sub-micrometer thickness values, dielectric breakdown is more likely to occur, leading to the occurrence of droplet hydrolysis, which, besides destroying the sample droplets, can cause substantial damages in the microfluidic chip.

Based on these final simulations and following the previous recommendations of Vieira *et al.*, (2017), Moita *et al.* (2018) and Jacinto *et al.* (2018), the final microfluidic chips should be coated with Teflon with a thickness between 1 and 6 μ m, which allows an efficient droplet motion with velocities up to 75mm/s, for a low applied voltage (below 90V) and low frequencies (9Hz). A simplified version of the device is schematically represented in Figure 2.

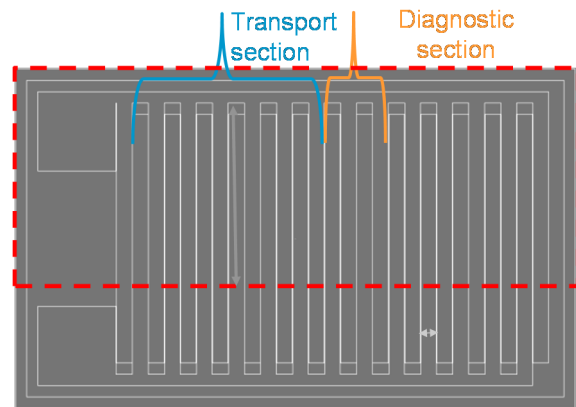


Figure 2: Simplified schematic of the microfluidic chip. Currently only the basic chips with the optimized electrodes size and configuration are being fabricated.

3.2 Analysis of the Suitability of the Analogue Fluids

The analogue fluids tested here are intended to mimic the actual biofluids to be assayed, namely in terms of the rheological properties, deformability and size of the particles. Despite having a shear-thinning behaviour, close to that of blood, the xanthan gum solutions cannot mimic the potential rheological modifications caused by cells deformation. In this context the polymeric suspensions provide a much more realistic approach. However, looking at the particles distribution within the fluid, with the confocal microscope, the images show a strong trend for the PMMA particles to agglomerate forming large rigid clusters, as illustrated in Figure 3.

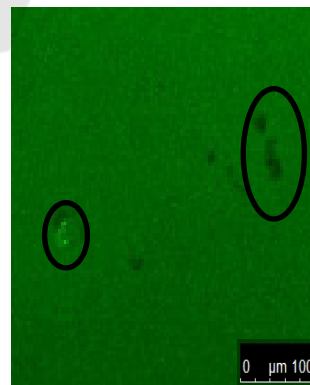
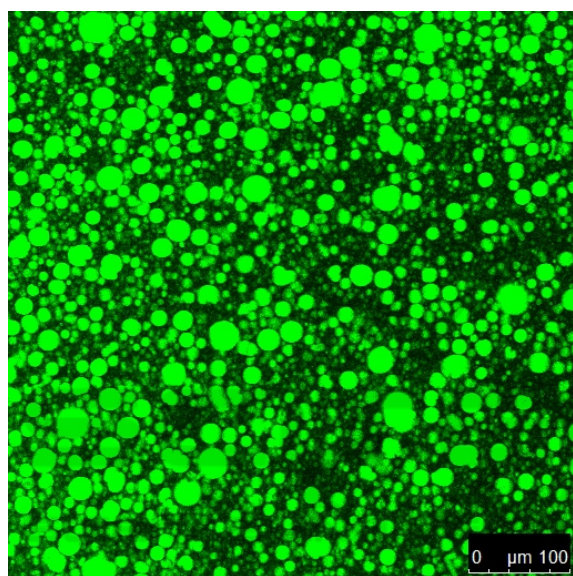


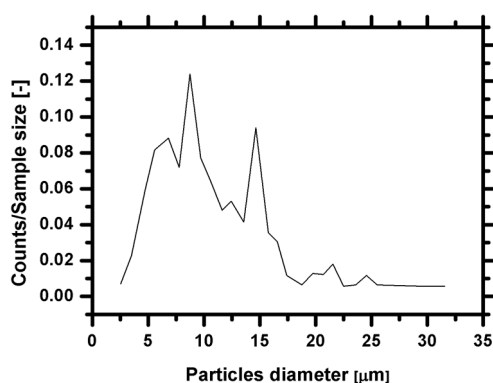
Figure 3: Illustrative image of the PMMA solution (with particles of characteristic size of 5 μ m) taken with the Laser Scanning Confocal Microscope (Leica SP8). The images were taken with an objective with 20X magnification and with a numerical aperture of 0.75.

For instance in the case illustrated in Figure 3, the characteristic size of the resulting particles is $5.46 \pm 0.38 \mu\text{m}$, but the agglomerates can be larger than $40 \mu\text{m}$. Also, the particles are approximately spherical, but the resulting agglomerates can depict quite irregular shapes.

On the other hand, the analogue fluid resulting from the addition of the surfactant is much more interesting in terms of the particles distribution, showing no evident agglomeration of the particles (Figure 4a), which also depict a spherical shape. The particle size distribution (which was evaluated for a sample of 170 particles) is slightly heterogeneous, as



a)



b)

Figure 4: a) Representative image of the analogue fluid prepared with the surfactant Brij40, obtained by Laser Scanning Fluorescent Confocal Microscopy (objective of 20x magnification and 0.75x numerical aperture). b) Size distribution of the semi-rigid particles obtained by image post-processing.

depicted in Figure 4b), but a simple filtering of the solution seems to considerably narrow the size distribution, homogenising the solution (Figure 5).

It is worth mentioning that having a particle size distribution more heterogeneous is in fact an advantage for the current study, since the pleural fluid samples may have different cells, with different morphologies, being the size distribution obtained here, similar to that reported by Tse *et al.* (2013) using pleural effusions.

The complete characterization of this kind of solutions is out of the scope of the present study and will be presented in a future work.

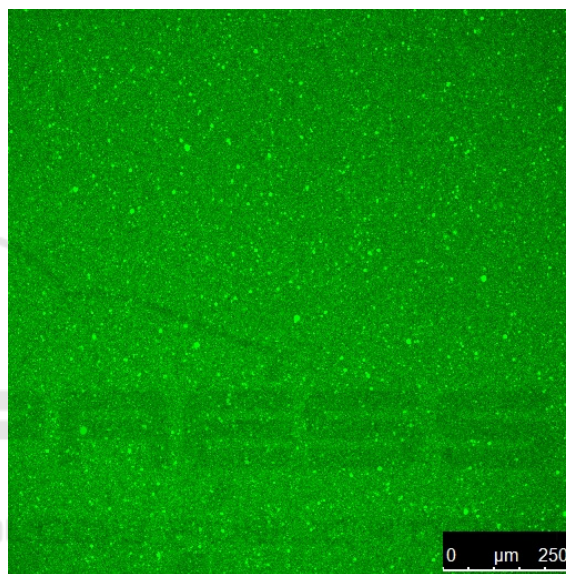


Figure 5: Representative image of the analogue fluid prepared with the surfactant, obtained by Laser Scanning Fluorescent Confocal Microscopy (objective of 20x magnification and 0.75x numerical aperture) after filtering the solution with a $10 \mu\text{m}$ filter.

After this brief analysis of the particles morphology and size distribution, it is now relevant to briefly check on their deformability, as they should be able to present similar stages of deformability, comparable to those of the sample cells. The deformation index DI, as initially defined in Pinho *et al.* (2013):

$$DI = \frac{L_{\text{major}} - L_{\text{minor}}}{L_{\text{major}} + L_{\text{minor}}} \quad (1)$$

where, L_{major} and L_{minor} refer to major and minor axis lengths of the cell was used to assess the deformability of the particles.

The range of maximum DI obtained with different particles is represented in Figure 6, which

includes results gathered from the work of Pinho (2018). The Figure shows a significant range of the deformation index, up to 0.5, particularly for semi-rigid particles, such as those obtained with the surfactant solution. As reported by Pinho *et al.* (2018) one may notice that the deformability of the rigid particles such as PMMA is lower than that of other analogues, including the semi-rigid particles obtained with the surfactant solution. Although the sizes of the particles used here are relatively narrow, the analogue solution with the surfactant can provide a wider range of particle diameters, as shown in Figure 4b). The detailed study of the particles deformability is out of the scope of the present work and will be presented in a different work.

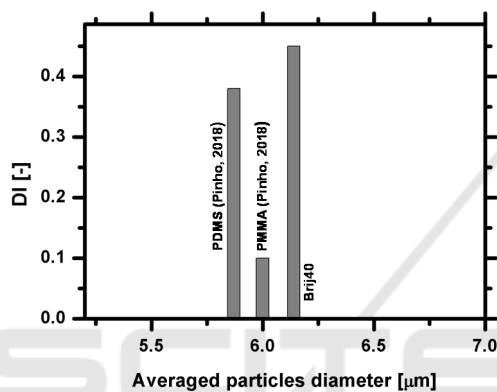


Figure 6: Deformation index DI as a function of the initial (averaged) particles diameter for the particles used in different analogue fluids.

The methodology used by Tse *et al.* (2013) for malignant diagnostics is quite complex and requires the establishment of different profiles, which are mainly different distributions of the deformability (which Tse *et al.*, 2013 defined as the ration $L_{\text{major}}/L_{\text{minor}}$), which is represented as a function of the initial diameter of the cells. Overall, considering that cell diameters in Tse *et al.* (2013) were ranging between 1 and $25\mu\text{m}$, this range of diameters is covered with our analogues, which show deformability ranges of the order of 1.25 or higher. This analysis must be adapted for our case study and for the various strategies that will be used to deform the cells, but these preliminary results suggest a good potential of these analogue fluids, and particularly the Brij40 solution to be used in our deformability studies.

Finally, given that our microfluidic device works under electrostatic actuation it is worth to analyse the electrostatic response of the analogue fluids. In this context Figure 7 depicts the variation of the equilibrium contact angle under actuation, as a

function of the applied voltage. The measurements were performed on a Teflon substrate, as described in section 2.2.1.

Figure 7 shows a clear response of all the analogue fluids tested here, under electrostatic actuation, as the contact angle decreases with the applied voltage, according to Young-Lippmann equation. The curves obtained here do not follow exactly Young-Lippmann equation since this classic theory does not take into account various phenomena such as energy dissipation and contact line saturation. These curves are in good qualitative agreement with those reported by Moita *et al.* (2016) taken with biofluids at similar experimental conditions.

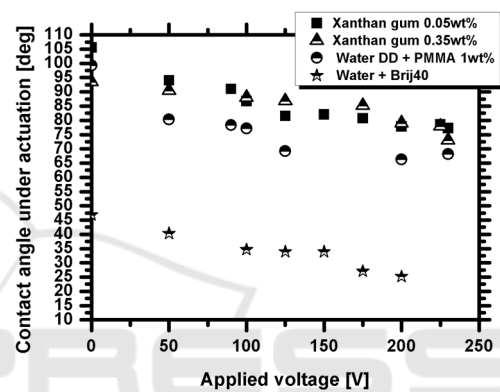


Figure 7: Electrostatic response of the analogue fluids: contact angle of an actuated droplet ($3\mu\text{l}$ of volume) deposited on a Teflon substrate, as a function of the applied voltage.

It is worth mentioning that the surfactant Brij40 solved in water significantly decreases the surface tension of the solution (Table 1), so the contact angles are much lower than those obtained with the other analogue fluids, which have surface tension values much closer to that of water. However, the dynamic response of the Brij40 solution to the electrostatic actuation is similar in magnitude to that depicted by the other analogue fluids, showing no evident signs of contact angle saturation for the highest applied voltages, contrarily to what is observed for instance in the xanthan gum solutions. Following these previous results, the Brij40 solution shows a high potential to be used as an analogue fluid in our study.

4 CONCLUSIONS

Following our previous work, this paper addresses the various steps required in the development of a

droplet based microfluidic device (based on electrostatic actuation) for early staged cancer diagnostics. The first part of the paper summarizes the steps followed up to now, towards the design and test of the microfluidic chip and discusses the final tests on the optimization of the materials, namely of the dielectric to be used as a coating material to our chip. Adsorption of the biomaterials has shown to be a relevant issue in our previous work. So, to overcome this problem, several analogue fluids are proposed and tested here, in an original approach, to infer on their suitability to be used in the test of the microfluidic device. The analogue fluids are characterized in terms of their main physico-chemical properties, the size distribution of the particles (mimicking the cells) and on their deformability, since the microfluidic device under development will explore the potential use of cell deformability to cancer diagnostics. The preliminary results discussed here suggest that a surfactant solution can be used as an analogue. The addition of the surfactant leads to the formation of semi-rigid particles with a size distribution (obtained by post-processing of images taken using Laser Scanning Fluorescent Confocal Microscopy), and deformability characteristics compatible with those of the biosamples to be studied.

ACKNOWLEDGEMENTS

The authors are grateful to Fundação para a Ciência e a Tecnologia (FCT) for financing the contract of A.S. Moita through the IF 2015 recruitment program (IF 00810-2015) and for partially financing this research through the exploratory project associated to this contract.

REFERENCES

Chim, J. C. R. M., 2015. Capillary biochip for point of use biomedical application, *MSc Thesis, Instituto Superior Técnico, Universidade de Lisboa*.

Cross, M. M., 1965. Rheology of non-Newtonian fluids: a new flow equation for pseudoplastic systems, *J. Colloid Sci.*, 20:417-437.

Dance, A., 2017. The making of a medical microchip. *Nature*, 545:512-514.

Geng, Hongyao, Feng, J., Stabryl, L. M., Cho, S. K., 2017 Dielectroetting manipulation for digital microfluidics: creating, transporting, splitting, and merging droplets. *Lab-on-Chip*, 17:1060-1068.

Gossett, D., Weaver, W., Mach, A., Hur, S., Tse, H., Lee, W., Amini H., Carlo, D., 2010. Label-free cell

separation and sorting in microfluidic systems, *Analytical and Bioanalytical Chemistry*, 397:3249-3267.

Hu, S., Wang, R., Tsang, C. M., Tsao, S. W., Sun, D., Lam, H. W., 2018. Revealing elasticity of largely deformed cells flowing along confining microchannels. *RSC Adv.*, 8:1030-1038.

Jacinto, F., Moita, A.S., Moreira, A.L.N., 2018. Design, test and fabrication of a droplet based microfluidic device for clinical diagnostics. In: *Proceedings of the 11th International Conference on Biomedical Electronics and Devices – Volume I: BIODEVICES 2018*, 19 – 21 January, Funchal, Madeira, pp. 88-95. ISBN 978-989-758-277-6.

Kato, M., Tanaka, A., Sasagawa, M., Adachi, H., 2008. Durable automotive windshield coating and the use thereof. *US Patent*, 8043421 B2.

Li, Y., Fu, Y. Q., Brodie, S. D., Alghane, M., Walton, A. J., 2012. Integrated microfluidics system using surface acoustic wave and electrowetting on dielectrics technology. *Biomicrofluidics*, 6:012812.

Lin, C. C., Wang, J. H., Wu, H. W., Lee, G. B., 2010. Microfluidic immunoassays. *JALA - J. Assoc. Lab. Autom.*, 15(3):253–274.

Moita, A. S., Herrmann, D, Moreira, A. L. N., 2015. Fluid dynamic and heat transfer processes between solid surfaces and non-Newtonian liquid droplets. *Applied Thermal Engineering*, 88:33-46.

Moita, A. S., Laurência, C., Ramos, J.A., Prazeres, D. M. F., Moreira, A. L. N., 2016. Dynamics of droplets of biological fluids on smooth superhydrophobic surfaces under electrostatic actuation, *J. Bionic Eng.*, 13:220-234.

Moita, A.S., Vieira, D., Mata, F., Moreira, A.L.N., 2018. Microfluidic devices integrating alternative clinical diagnostic techniques based on cell mechanical properties. *Biomedical Engineering Systems and Technologies. Series: Communications in Computer and Information Science, Chapter 4: Microfluidic Devices Integrating Clinical Alternative Diagnostic Techniques Based on Cell Mechanical Properties*, N. Peixoto et al. (Eds.), Springer International Publishing AG, part of Springer Nature, 881, pp. 74-93.

Mugele, F, Baret, J.C., 2005. Electrowetting: From basics to applications. *J. Phys. Condensed Mat.*, 17:R705–R774.

Nelson, W.C., Kim, C.-j., 2012. Droplet actuation by Electrowetting-on-Dielectric (EWOD): A review. *J. Adhesion Sci. Tech.*, 26, 1747-1771.

Pinho, D. M. D., 2018. Blood rheology and red blood cell migration in microchannel flow. PhD Thesis. Faculdade de Engenharia da Universidade do Porto.

Pinho, D., Yaginuma, T., Lima, R., 2013. A microfluidic device for partial cell separation and deformability assessment. *BioChip Journal*, 7(4):pp 367-374.

Pollack, M. G., Pamula, V.K., Srinivasan, V., Eckhardt, A.E., 2011. Applications of electrowetting-based digital microfluidics in clinical diagnostics, *Expert Ver. Molecular Diagnostics*, 11(4):397-407.

- Restolho, J., Mata, J. L., Saramago, B., 2009. Electrowetting of ionic liquids: contact angle saturation and irreversibility. *J. Phys. Chem C*, 113: 9321–9327.
- Shields I. V., Reyes, C. D., López, G. P., 2015. Microfluidic cell sorting: A review of the advances in the separation of cells from debulking to rare cell isolation, *Lab on a Chip*, 16:1230–1249.
- Takahashi, K., Hattori, A., Suzuki, I., Ichiki, T., 2004. Non-destructive on-chip cell sorting system with real-time microscopic image processing, *Journal of Nanobiotechnology*, 2:1-8.
- Tse, H. T. K., Gossett, D. R., Moon, Y. S., Masaeli, M., Sohsman, M., Ying, Y., Mislick, K., Adam, R. P., Rao, J. Di Carlo, D., 2013. Quantitative diagnosis of malignant pleural effusions by single-cell mechanophenotyping, *Science Translational Medicine*, 5(212): 212ra163.
- Vieira, D. Mata, F., Moita, A.S., Moreira, A.L.N., 2017. Microfluidic Prototype of a Lab-on-Chip Device for Lung Cancer Diagnostics. *Proceedings of the 10th International Joint Conference on Biomedical Engineering Systems and Technologies - Volume 1: BIODVICES*, 63-68, 2017, Porto, Portugal, 21-13 February 2017. DOI: 10.5220/0006252700630068, ISBN: 978-989-758-216-5.
- Zeggari, R., Manceau, J. F., Aybeke, E. N., Yahiaoui, E., Boireau, E. L., 2014. Design and fabrication of an acoustic micromixer for biological media activation, *Procedia Engineering*, 87:935-938.

